Chemistry–A European Journal

Supporting Information

Polymorphs of the Gadolinite-Type Borates ZrB_2O_5 and HfB_2O_5 Under Extreme Pressure

Anna Pakhomova[+],*[a] Birgit Fuchs[+],[b] Leonid S. Dubrovinsky,[c] Natalia Dubrovinskaia,[d, e] and Hubert Huppertz*[b]

Table of contents

Experimental Procedures

Synchrotron measurements

In situ high-pressure single-crystal diffraction experiments (SCXRD) were performed at the experimental station P02.2 (Extreme Conditions Beamline) at the synchrotron Petra III (Hamburg, Germany). Symmetric diamond anvil cells (DACs) with culets diameter of 150 μm were used for pressure generation. The sample chamber with an approximate diameter of 75 μm was obtained by drilling the preindented (up to ~20 μm) rhenium gasket. Preselected single-crystals of β-ZrB_2O_5 and β-HfB_2O_5 were placed inside the sample chamber along with a ruby sphere for pressure estimation. The DAC was loaded with neon as pressure-transmitting medium using the in-house gas loading system at Petra III. Monochromatic X-ray diffraction experiments were performed using X-rays with a wavelength of ~0.29 Å. The X-ray beam was focused to ~2×2 μm^2 by Kirkpatrick-Baez mirrors. Diffraction patterns were collected using a Perkin Elmer 1621 detector. Before the experiment, the detector-sample-distance, coordinates of the beam center, tilt angle, and tilt plane rotation angle of the detector images were calibrated with a CeO_2 standard using the procedure implemented in the program Dioptas.[1]

At each pressure, both a wide-scan and a stepped ω-scan were collected for each crystal. The wide-scans consisted of 40 s exposures during rotations of ± 20° of the DAC, while the step scans consisted of individual exposures taken with 0.5° intervals over the entire opening angle of the cell of 32°. For the analysis of the single-crystal diffraction data (indexing, data integration, frame scaling and absorption correction), the CrysAlisPro software package was used. A single-crystal of an orthoenstatite ($(Mg_{1.93},Fe_{0.06})(Si_{1.93},Al_{0.06})O_6$, *Pbca*, a = 8.8117(2), b = 5.18320(10), c = 18.2391(3) Å), was used to calibrate the instrument model in the CrysAlisPro software (sample-to-detector distance, the detector's origin, offsets of the goniometer angles and rotation of the X-ray beam and the detector around the instrument axis).

Single-crystal X-ray diffraction refinement

The crystal structures of the new compounds γ-ZrB_2O_5 and γ-HfB_2O_5 were determined by the dual space method using the SHELXT software.[2] After the structure solution, most of the atoms were found and the remaining were located from a series of difference Fourier maps. The crystal structures were refined against F^2 on all data by full-matrix least squares with the SHELXL software.[3]

Results and Discussion

Table S1. Crystallographic data and refinement parameters for β-ZrB_2O_5 for all pressure steps.

Pressure, GPa	2.2	16.01	23.8	33.8	43.68	53.9	69.3	75	79.3	85.4	89.7	94.6	100.6	105	109.4	114.3	119.6
Space group									$P2_1/c$								
a, Å	4.377(1)	4.292(1)	4.247(1)	4.199(1)	4.155(1)	4.115(1)	4.060(1)	4.040(1)	4.026(1)	4.005(1)	3.988(1)	3.969(1)	3.965(1)	3.956(1)	3.951(1)		3.901(2)
b, Å	6.903(1)	6.811(1)	6.769(1)	6.715(1)	6.666(1)	6.609(1)	6.575(1)	6.534(1)	6.519(1)	6.513(1)	6.502(1)	6.497(1)	6.466(1)	6.432(1)	6.426(2)		6.434(2)
c, Å	8.948(1)	8.800(1)	8.726(1)	8.644(1)	8.564(1)	8.498(1)	8.41(2)	8.377(1)	8.352(1)	8.31(1)	8.294(1)	8.270(1)	8.245(1)	8.232(1)	8.200(1)		8.110(4)
β, deg	90.99(1)	91.38(1)	91.61(1)	91.83(1)	91.99(1)	92.03(1)	92.39(2)	92.41(1)	92.47(1)	92.75(2)	92.63(1)	92.75(2)	92.72(2)	92.77(2)	93.01(2)		92.95(8)
V, Å^3	270.27(2)	257.15(3)	250.78(2)	243.45(2)	237.05(3)	230.98(3)	224.24(6)	220.90(2)	218.96(3)	216.66(3)	214.82(3)	212.99(5)	211.13(5)	209.21(4)	207.88(6)		203.3(1)
Z									4								
Data collection and refinement																	
Wavelength, Å									0.2901								
Max. θ, deg	18.228	17.958	18.102	18.274	18.123	18.217	11.101	18.184	17.648	17.270	18.005	17.568	17.598	17.663	17.699		12.833
R_1, all data	0.0273	0.0711	0.0529	0.0476	0.0281	0.0516	0.0452	0.0396	0.0272	0.0634	0.0366	0.0415	0.0504	0.0465	0.0723		0.1027
R_1, $I > 2\sigma(I)$	0.0266	0.0704	0.0523	0.0454	0.0271	0.0505	0.0439	0.0383	0.0266	0.0627	0.0354	0.0402	0.0491	0.0440	0.0679		0.0826
wR_2, all data	0.0725	0.1806	0.1529	0.1156	0.0734	0.1517	0.1276	0.0994	0.0715	0.1694	0.0998	0.1114	0.1263	0.1194	0.1836		0.2302
wR_2, $I > 2\sigma(I)$	0.0706	0.1769	0.1506	0.1129	0.0721	0.1492	0.1260	0.0968	0.0707	0.1982	0.0975	0.1096	0.1239	0.1132	0.1737		0.2066
GooF	1.117	1.078	1.110	1.044	1.083	1.117	1.197	1.057	1.087	1.158	1.036	1.078	1.077	1.095	1.043		1.075

Table S2. Crystallographic data and refinement parameters for β-HfB_2O_5 for all pressure steps.

Pressure, GPa	2.2	16.01	23.8	33.8	43.68	53.9	69.3	75	79.3	85.4	89.7	94.6	100.6	105	109.4	114.3	119.6
Space group									$P2_1/c$								
a, Å	4.360(1)	4.280(1)	4.240(1)	4.192(1)	4.156(1)	4.122(1)	4.071(1)	4.044(1)	4.033(1)	4.024(1)	4.006(1)	3.989(1)	3.966(1)	3.939(1)	3.924(1)	3.892(1)	3.872(1)
b, Å	6.881(1)	6.797(1)	6.754(1)	6.704(1)	6.672(1)	6.643(1)	6.607(1)	6.581(1)	6.578(1)	6.585(1)	6.583(1)	6.581(1)	6.568(1)	6.530(2)	6.510(1)	6.431(1)	6.410(1)
c, Å	8.943(1)	8.787(1)	8.696(1)	8.608(1)	8.488(1)	8.370(1)	8.264(1)	8.230(1)	8.186(1)	8.11(1)	8.080(1)	8.06(1)	8.05(2)	8.07(2)	8.08(2)	8.168(2)	8.18(2)
β, deg	90.82(1)	91.26(1)	91.41(1)	91.61(1)	91.61(1)	92.20(2)	92.26(2)	92.46(2)	92.45(2)	92.75(2)	92.75(2)	92.79(2)	92.91(3)	93.18(4)	93.15(4)	92.90(4)	92.92(6)
V, Å^3	268.27(8)	255.54(9)	248.95(9)	241.76(2)	235.22(2)	229.0(2)	222.1(2)	218.8(2)	217.0(2)	214.8(3)	212.8(2)	211.3(3)	209.4(3)	207.2(5)	206.1(4)	204.2(4)	202.8(6)
Z									4								
Data collection and refinement																	
Wavelength, Å									0.2901								
Max. θ, deg	18.294	17.865	18.022	17.260	17.507	17.697	13.069	17.418	17.466	17.270	17.336	17.240	17.289	17.216	17.270	17.462	17.521
R_1, all data	0.0302	0.0457	0.0336	0.0539	0.0372	0.0540	0.0406	0.0555	0.0257	0.0325	0.0311	0.0530	0.0522	0.0758	0.0548	0.0280	0.0573
R_1, $I > 2\sigma(I)$	0.0295	0.0445	0.0324	0.0530	0.0366	0.0526	0.0385	0.0549	0.0249	0.0318	0.0308	0.0521	0.0498	0.0735	0.0529	0.0272	0.0564
wR_2, all data	0.0798	0.1203	0.0873	0.1509	0.1073	0.1423	0.1082	0.1588	0.0637	0.0954	0.0822	0.1492	0.1471	0.2339	0.1681	0.742	0.1482
wR_2, $I > 2\sigma(I)$	0.0791	0.1171	0.0860	0.1501	0.1069	0.1390	0.1064	0.1577	0.0631	0.0945	0.0819	0.1471	0.1437	0.2285	0.1647	0.729	0.1466
GooF	1.143	1.128	1.172	1.153	1.199	1.188	1.198	1.217	1.131	1.132	1.066	1.073	1.163	1.142	1.191	1.091	1.125

Table S3. Interatomic B–O distances /Å for β-ZrB_2O_5 and β-HfB_2O_5 at 119.6 GPa (standard deviations in parentheses).

β-ZrB_2O_5					
B1	–O4	1.28(9)	B2	–O2	1.36(4)
	–O2	1.33(5)		–O1	1.39(5)
	–O3	1.33(9)		–O3	1.4(1)
	–O5	1.33(5)		–O4	1.72(2)
Ø		**1.32**	**Ø**		**1.47**
β-HfB_2O_5					
B1	–O5	1.35(1)	B2	–O1	1.352(6)
	–O3	1.36(2)		–O2	1.360(6)
	–O2	1.37(2)		–O3	1.38(2)
	–O4	1.39(2)		–O4	1.45(2)
Ø		**1.37**	**Ø**		**1.38**

Table S4. Bond angles /deg for β-ZrB_2O_5 and β-HfB_2O_5 at 119.6 GPa (standard deviations in parentheses).

β-ZrB_2O_5			
O4–B1–O3	92(3)	O2–B2–O4	91(5)
O2–B1–O5	105(3)	O1–B2–O4	102(6)
O2–B1–O3	108(3)	O3–B2–O4	104(4)
O4–B1–O5	113(4)	O2–B2–O3	116(6)
O4–B1–O2	115(8)	O2–B2–O1	118(3)
O5–B1–O3	125(8)	O1–B2–O3	118(5)
Ø	**110**	**Ø**	**108**
β-HfB_2O_5			
O2–B1–O4	100.0(6)	O2–B2–O4	99(1)
O5–B1–O2	105.9(5)	O3–B2–O4	104.1(6)
O2–B1–O4	106(2)	O1–B2–O4	112(2)
O3–B1–O2	110.8(6)	O2–B2–O3	112(2)
O5–B1–O4	112.6(8)	O1–B2–O3	113(1)
O5–B1–O3	120(2)	O1–B2–O2	115.3(4)
Ø	**109**	**Ø**	**109**

Table S5. Charge distributions according to the CHARDI ($\sum Q$) concept.

γ-ZrB_2O_5	Zr1	B1	B2	O1	O2	O3	O4	O5
$\sum Q$	4.07	2.91	3.02	-2.09	-2.04	-1.72	-1.94	-2.21
γ-HfB_2O_5	Hf1	B1	B2	O1	O2	O3	O4	O5
$\sum Q$	4.06	2.94	3.00	-1.94	-2.13	-2.07	-2.21	-1.64

Table S6. Cation radii (r) and bulk moduli (K_0) of the cation polyhedra in the crystal structures of datolite, hingganite-(Y), and β-ZrB_2O_5.

	MO_8			$T1O_4$			$T2O_4$			Unit cell
	M	r /Å[6]	K_0 /GPa	T1	r /Å[6]	K_0 /GPa	T2	r /Å[6]	K_0 /GPa	K_0 /GPa
Datolite[4]	Ca^{2+}	1.12	76(5)	Si^{4+}	0.26	325(14)	B^{3+}	0.11	314(34)	106(4)
Hingganite-(Y)[5]	Y^{3+}	1.019	118(5)	Si^{4+}	0.26	283(28)	Be^{2+}	0.27	212(19)	124(1)
β-ZrB_2O_5*	Zr^{4+}	0.84	242(5)	B^{3+}	0.11	350(10)	B^{3+}	0.11	470(11)	228(1)

* The evolution of the unit cell volume and polyhedral volumes as a function of pressure was fit using second-order Birch-Murnaghan equation of state.

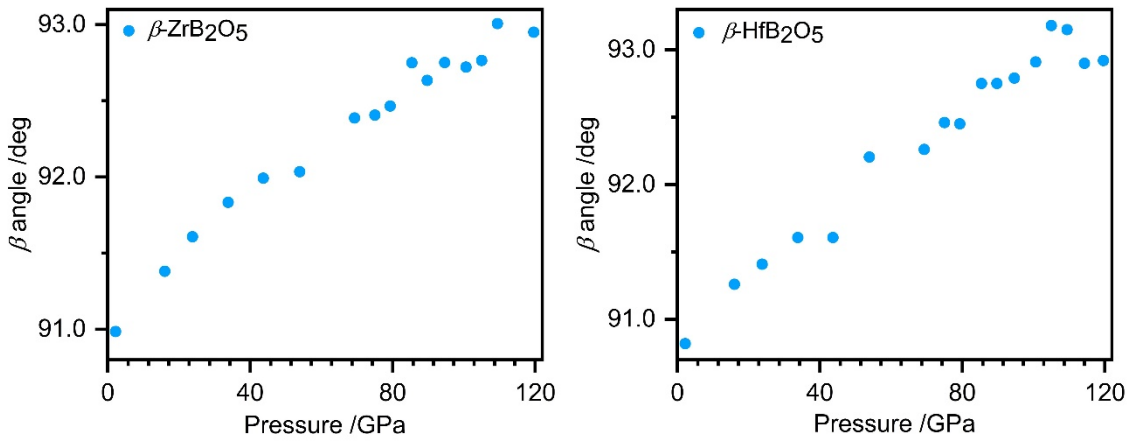

Figure S1. Development of the β angle in β-ZrB_2O_5 (left) and β-HfB_2O_5 (right).

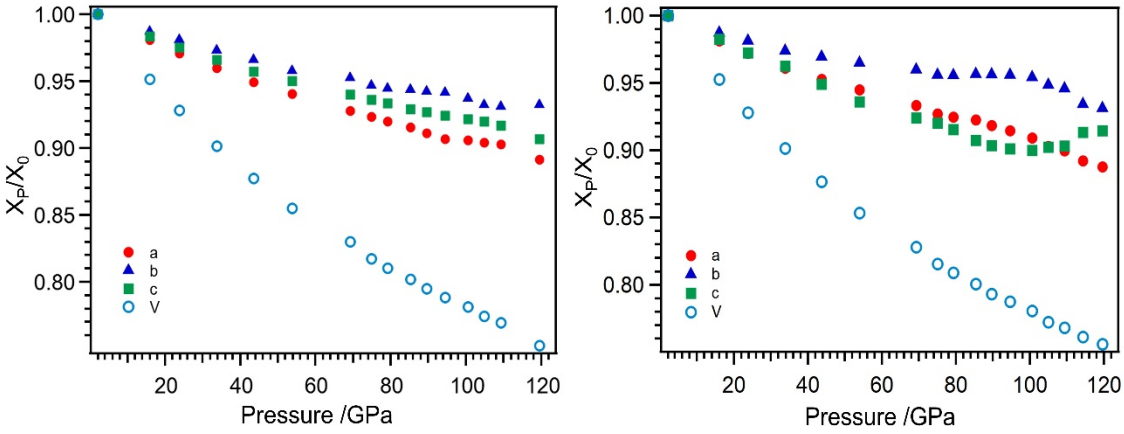

Figure S2. Normalized unit cell parameters for ZrB_2O_5 (left) and HfB_2O_5 (right).

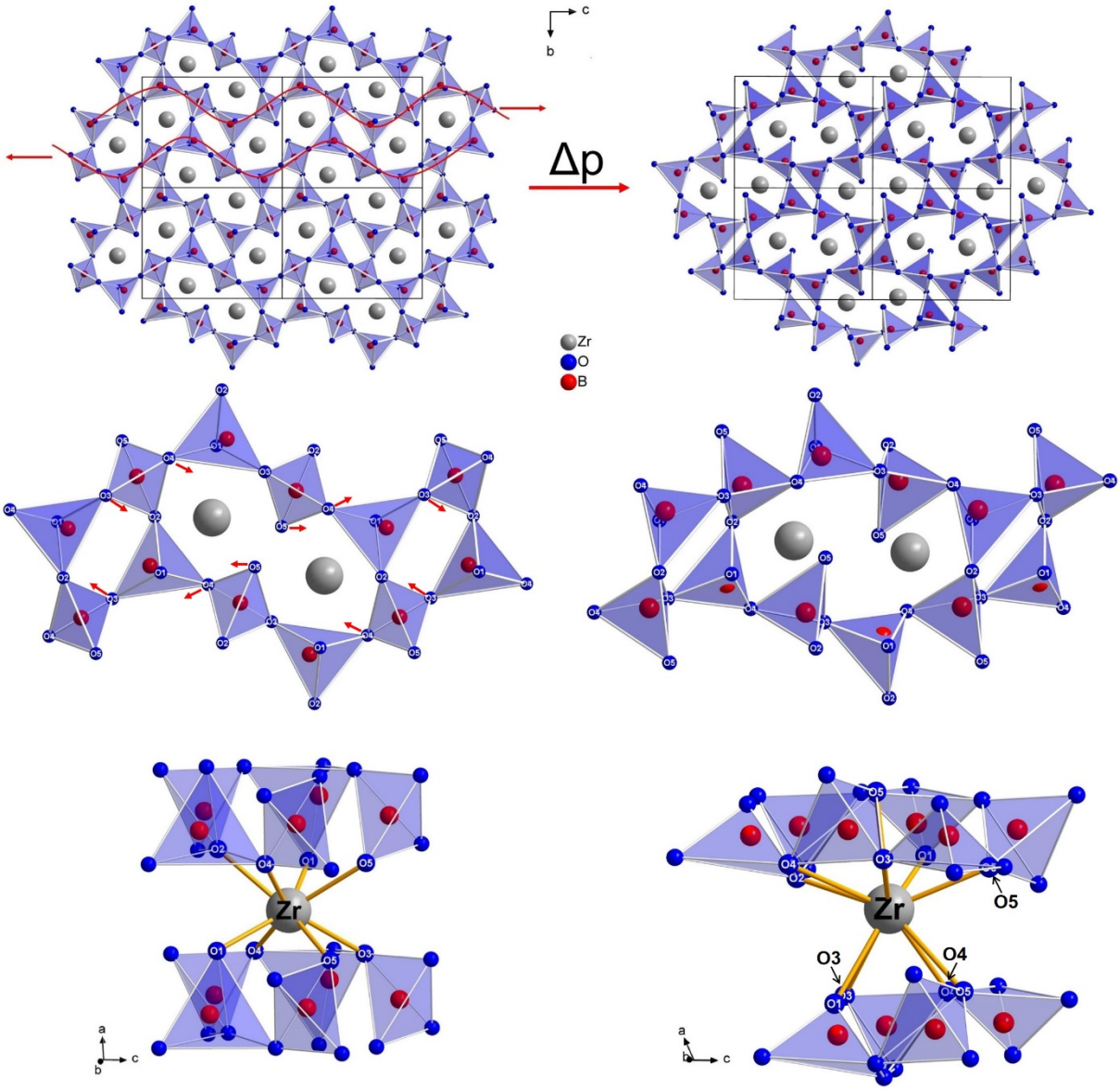

Figure S3. Displacive phase transition from β-ZrB_2O_5 (left) to γ-ZrB_2O_5 (right) at high pressure. Top: The BO_4 tetrahedra along the wavelike arrangement (marked red on the right) orient themselves in direction of the red arrows. Middle: Comparison of the four- and eight-membered rings. Red arrows indicate the shift caused by the transition from β- to γ-phase. Bottom: Coordination of the Zr^{4+} cation between the layers (the γ-phase was transformed into the space group $P2_1/c$ for a better comparison).

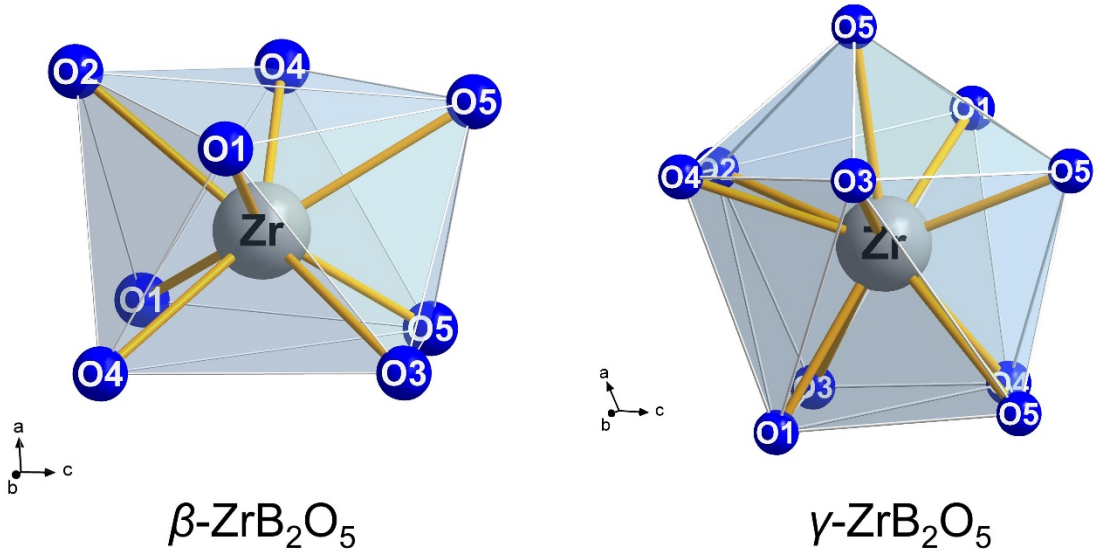

Figure S4. Comparison of the Zr^{4+} coordination in β-ZrB_2O_5 (eightfold; left) and γ-ZrB_2O_5 (tenfold; right).

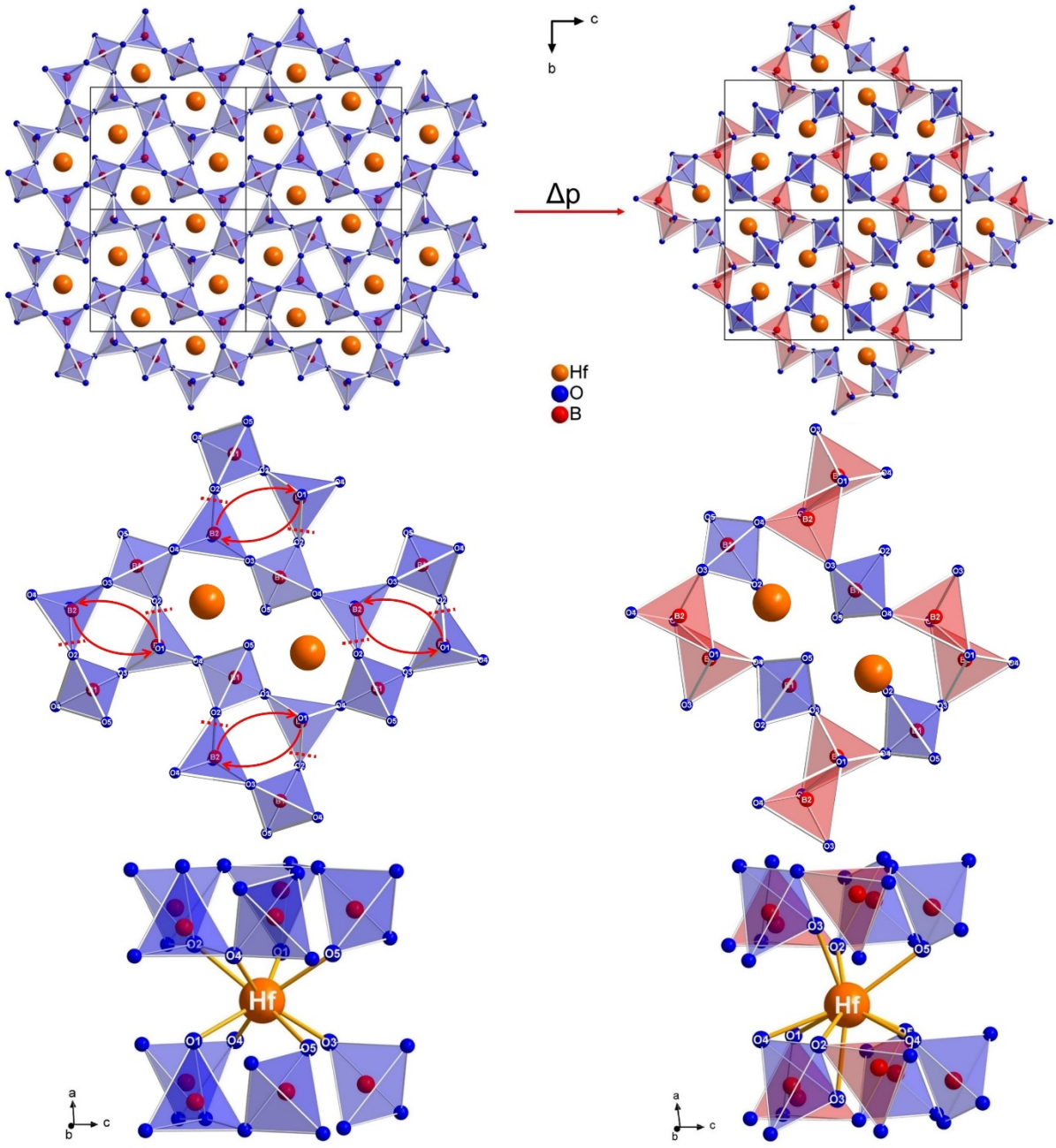

Figure S5. Top: Reconstructive phase transition from β-HfB_2O_5 (left) to γ-HfB_2O_5 (right) at high pressure. Middle: Red dotted lines indicate the bonds that are broken during the phase transition. Red arrows show the formation of new bonds between B2 and O1 atoms that subsequently form the edge-sharing BO_4 tetrahedra. Bottom: Coordination of the Hf^{4+} cation between the layers.

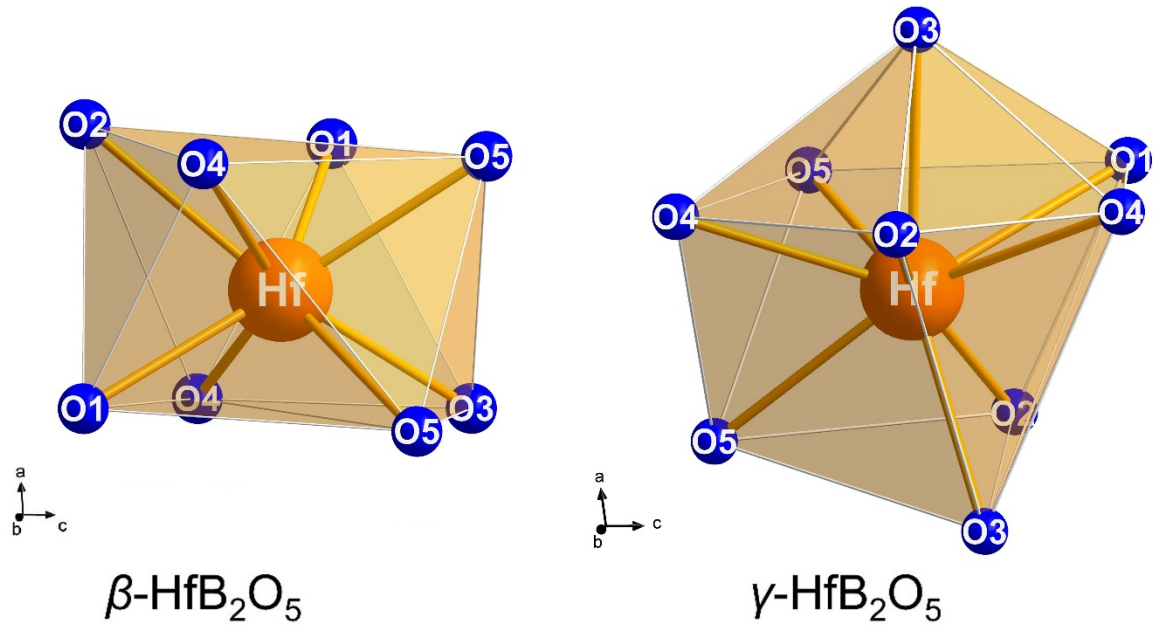

Figure S6. Comparison of the Hf^{4+} coordination in β-HfB_2O_5 (eightfold; left) and γ-HfB_2O_5 (ninefold; right).

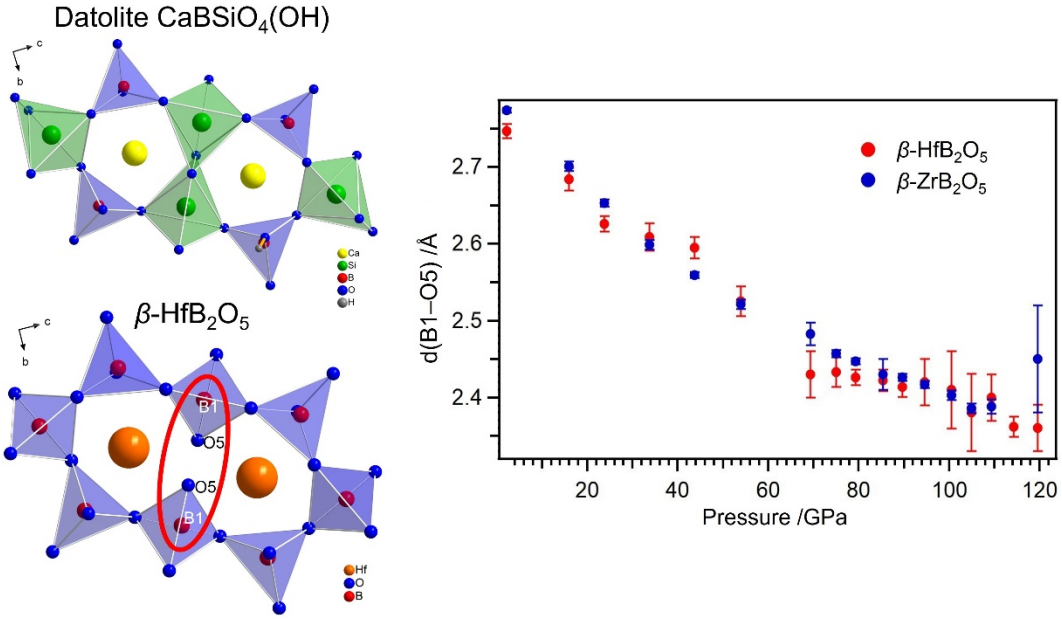

Figure S7. Comparison of the resulting five-membered rings in datolite (top left) and the remaining eight-membered ring in β-HfB_2O_5 (bottom left) and evolution of the B1–O5 distance in β-ZrB_2O_5 and β-HfB_2O_5 (right).

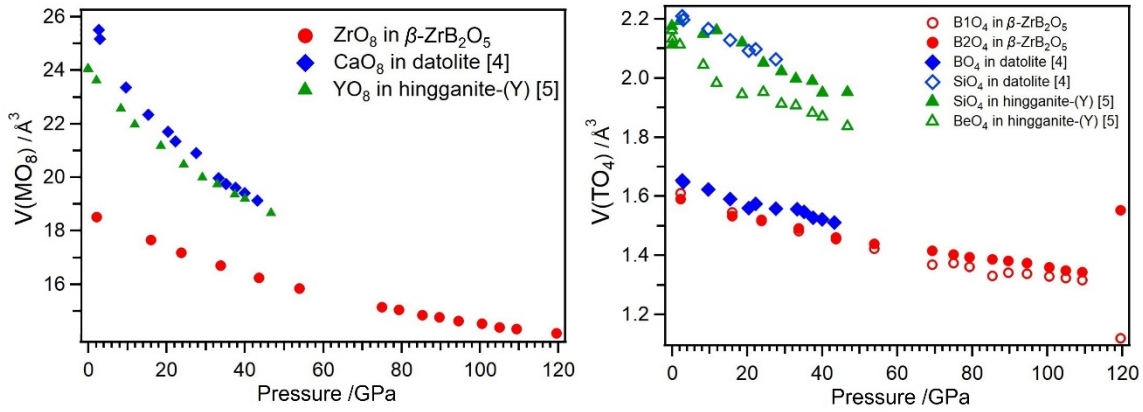

Figure S8. Pressure dependencies of the volumes of the MO_8 (M = Zr, Ca, Y; left) and TO_4 (T = Si, Be, B; right) coordination polyhedra in the crystal structures of β-ZrB_2O_5, datolite $CaBSiO_4(OH)$,[4] and hingganite-(Y) $YBeSiO_4(OH)$.[5]

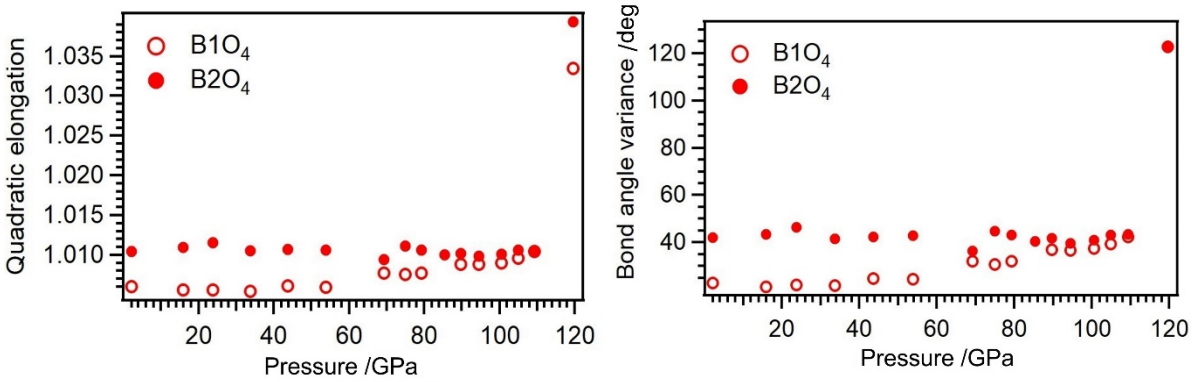

Figure S9. The evolution of the quadratic elongation (QE; left) and bond angle variance (BAV, deg; right) of the BO_4 tetrahedra along the compression of β-ZrB_2O_5. The parameters QE and BAV show the deviation of TO_4 polyhedra from the ideal tetrahedral geometry and are defined as: $\mathrm{QE} = \frac{1}{4}\sum_{i=1}^{4}\left(\frac{l_i}{l_0}\right)^2$ and $\mathrm{BAV} = \sqrt{\frac{1}{5}\sum_{i=1}^{6}(\theta_i - 109.47)^2}$ where l_0 is a center-to-vertex distance for the ideal tetrahedron whose volume is equal to that of the distorted tetrahedron with bond lengths l_i and bond angles θ_i.[6]

References

[1] C. Prescher, V. B. Prakapenka, *High Pressure Res.* **2015**, *35*, 223-230.

[2] G. M. Sheldrick, *Acta Crystallogr.* **2015**, *C71*, 3-8.

[3] G. M. Sheldrick, *Acta Crystallogr.* **2008**, *A64*, 112-122.

[4] L. A. Gorelova, A. S. Pakhomova, G. Aprilis, L. S. Dubrovinsky, S. V. Krivovichev, *Inorg. Chem. Front.* **2018**, *5*, 1653–1660.

[5] L. A. Gorelova, A. S. Pakhomova, S. V. Krivovichev, A. V. Kasatkin, L. S. Dubrovinsky, *Phys. Chem. Minerals* **2020**, *47*, 22.

[6] K. Robinson, G. V. Gibbs, P. H. Ribbe, *Science* **1971**, *172*, 567-570.